

Colorimetric detection of bisphenol A in food and water based on the laccase-mimicking activity of silver phosphate nanoparticles

Siyu Wu¹, Jiali Chen¹, Yue Tang² and Yuangen Wu^{1,2*} ¹ School of Liquor and Food Engineering, Guizhou University, Guiyang 550025, China² College of Life Sciences, Guizhou University, Guiyang 550025, China* Corresponding author, E-mail: wuyg1357@163.com; ygwu@gzu.edu.cn

Abstract

Bisphenol A widely remains in food and environmental systems. A small amount of bisphenol A can directly affect human health. However, the recent colorimetric detection methods of bisphenol A still meet the challenges such as complex operations and the influence of high-salt solutions, resulting in inaccurate detection results. Herein, Ag₃PO₄ nanoparticles are prepared through a facile coprecipitation method and have excellent laccase-mimicking catalytic activity. Under the catalytic action of Ag₃PO₄ nanoparticles, bisphenol A loses electrons and further reacts with 4-amino-antipyrine to form a red substance. Thus, a novel rapid colorimetric method for bisphenol A detection is first established based on the laccase-mimicking activity of Ag₃PO₄ nanoparticles. The limit of detection of the colorimetric method is determined as low as 0.222 mg·L⁻¹, which is lower than the National Health and Family Planning Commission of China and the United States Food and Drug Administration. Moreover, the colorimetric method displays excellent selectivity against other competitive targets. Further research has confirmed the accuracy, reliability, and rapidity of the colorimetric method for detecting bisphenol A in actual food and water samples, which indicates that such a colorimetric method will play a potentially vital role in practical applications.

Citation: Wu S, Chen J, Tang Y, Wu Y. 2025. Colorimetric detection of bisphenol A in food and water based on the laccase-mimicking activity of silver phosphate nanoparticles. *Food Innovation and Advances* 4(1): 73–82 <https://doi.org/10.48130/fia-0025-0008>

Introduction

Bisphenol A (BPA) is one of the most produced and consumed chemicals in the world, which has penetrated people's daily lives in many ways^[1], such as most food contact materials, electronic devices, water pipes, etc^[2]. Thus, BPA is easy to remain in food and environmental systems^[1]. A small amount of BPA can directly affect human health, leading to diseases such as thyroid damage, diabetes, cardiovascular damage, high blood pressure, and cancer^[3]. To avoid the potential health risks, the National Health and Family Planning Commission of China (NHFPC) stipulates the migration amount should not exceed 0.6 mg·kg⁻¹ when BPA is used in food contact plastics, coatings, and adhesives [GB 9685-2016]. While the United States Food and Drug Administration (FDA) has defined the maximum residue limit of BPA in polycarbonate drinking utensils as 1,000 mg·kg⁻¹ (content requirement). Currently, high-performance liquid chromatography (HPLC), liquid chromatography-mass spectrometry (LC-MS), and gas chromatography-mass spectrometry (GC-MS) are the main methods for BPA detection, which have the advantages of accurate results and high sensitivity. For instance, Su and coworkers applied a novel solid phase extraction adsorbent for chromatographic analysis, which provides optimal resolution between target analytes, cleaning BPA up and separating it from the column to detect BPA concentration in food^[4]. However, the chromatography-based methods are usually time-consuming, cumbersome, and require large-scale precision instruments^[5], which are difficult to meet the needs of rapid detection of BPA^[6,7].

Recently, the rapid detection methods of BPA mainly focused on fluorescence, electrochemistry, and colorimetry. Most fluorescence methods usually quench the fluorescence of quantum dots directly^[8,9] or proteases after the formation of BPA-protease complexes^[10]. The fluorescence emission of silicon nanoparticles (SiNPs) can be quenched by BPA products oxidized by horseradish

peroxidase (HRP) and H₂O₂, thus BPA concentration can be analyzed by the change of fluorescence intensity^[11]. However, quantum dots and proteases are highly susceptible to environmental influences, which limits the practical application of fluorescence methods. The principle of the electrochemical method is generating potential difference or current change^[12] when BPA binds to biometric molecules^[13] such as antibodies^[14] and aptamers^[15]. The modified Cu-CD/NH electrode can oxidize the phenol hydroxyl group and output a strong electrochemical signal so that BPA quantity can be measured by the change of current value^[16]. However, the operation of electrochemistry is complex, and organic solvents^[17] are usually used for the treatment of electrodes. Besides, the stability of electrode materials is easily affected by environmental factors such as temperature and pH, which greatly limits its application in practical detection^[12]. The colorimetric method is one of the best techniques to overcome the above disadvantages^[18], converting color change into a sensing signal, which has the advantages of easy operation, visual observability^[19], high sensitivity, excellent selectivity, and high precision^[20]. The designed dual-mode biosensor is precise with the participation of colorimetry, which improves the selectivity and sensitivity of the sensor^[21,22]. Recently, several colorimetric methods such as smartphone-based portable spectrometers^[23], Spiegelmer-driven colorimetric biosensors, and a colorimetric aptamer sensor have been used for BPA detection^[24]. To date, the most common strategy for colorimetric detection of BPA is the aggregation of gold nanoparticles (AuNPs) mediated by aptamers to produce color changes^[25,26]. However, AuNPs are easily affected by high-salt solutions to form irreversible aggregation, resulting in inaccurate detection results^[27]. Therefore, it is greatly significant to develop a colorimetric signal carrier with high stability and simple preparation for the on-site detection of BPA.

Laccase belongs to a family of oxidases that contain copper and possesses the ability to catalyze the degradation of various

refractory organic contaminants^[28,29]. Because only water is generated as a byproduct during the catalytic process, laccase exhibits high environmental friendliness^[30]. Natural laccase has disadvantages such as low yield, low activity, difficulty in purification, and easy inactivation at high temperatures, which limit the further application in the degradation and analysis of pollutants^[31]. Consequently, researchers have tried to develop laccase mimics as low-cost and highly stable alternatives to natural laccase^[32]. Recently, nanozymes have attracted much attention from researchers. They have various superiorities such as high stability, excellent catalytic activity, and low cost^[33,34], widely applied in hazard detection, environmental control, industrial production, and other fields^[35]. For example, the CeO₂-MIL (Fe) metal-organic framework is used in the detection of melamine and mercury ions^[36]. Currently, an enzyme with laccase-mimicking activity is mostly used to detect phenolic compounds^[37,38] such as 2,4-dichlorophenol (2,4-DP), chlorophenol, and dopamine^[39,40]. For example, an amorphous CA-Cu enzyme with laccase-like activity was successfully prepared and then used for the breakdown of chlorophenol and diphenol, as well as for detecting dopamine^[41]. Unfortunately, colorimetric detection of BPA based on nanomaterials with laccase-mimicking activity is rarely reported. Hence, it is of great significance to prepare a novel rapid colorimetric strategy for BPA analysis using laccase mimics.

Herein, silver phosphate nanoparticles (Ag₃PO₄ NPs) are prepared through a simple precipitation method and possess excellent laccase-mimicking activity. BPA as a substrate can be catalyzed by Ag₃PO₄ NPs to generate red products, which enables us to create an uncomplicated, fast, and stable method for colorimetric detection of BPA. The proposed colorimetric method can be conveniently and quantitatively used for BPA detection, which has achieved good results in actual sample testing. The colorimetric system developed in this research offers a novel approach for detecting hazardous phenolic compounds, also broadening the utilization of food analysis for nanomaterials with laccase-like activity.

Materials and methods

Reagents and chemicals

Laccase (≥ 0.5 U/mg, from *Trametes versicolor*), Bisphenol A (BPA), Bisphenol AF (BPAF), Bisphenol B (BPB), AgNO₃, Na₂HPO₄, 2,4-dichlorophenol (2,4-DP), phenol, catechol, 3-aminophenol, 2-nitroresorcinol, 4-amino-antipyrine (4-AAP), N-(2-Hydroxyethyl) piperazine-N'-2-ethanesulfonic acid (HEPES) ($\geq 98.0\%$), anhydrous ethanol ($\geq 99.5\%$), glucose, CaCl₂, KCl, CuSO₄, FeCl₃·6H₂O, p-Nitrophenol, 4-aminophenol, tyrosine, leucine, phenylalanine, lysine, serine and all standard solution of heavy metals are purchased from Aladdin Co., LTD. (Shanghai, China). The 96-well microplates are purchased from NEST Biotechnology Co., Ltd. (Wuxi, China). All reagents utilized are of at least analytically pure grade ($\geq 99.0\%$) and necessitate no additional purification or treatment. The experimental water used is double-distilled.

Instrumentation

A field emission scanning electron microscope (FESEM) SU8010 (Hitachi, Japan) is used to measure the morphology and size of the Ag₃PO₄ nanomaterials. UV/vis spectra and absorbance values are recorded by the Microplate Spectrophotometer Varioskan Flash and Multiskan SkyHigh (Thermo Scientific, USA). LC-MS/MS SCIEX Triple Quad™ 3500 LC-MS/MS (SCIEX, USA) was applied to analyze the content of BPA in food and water.

Synthesis of Ag₃PO₄ NPs

Ag₃PO₄ NPs have been synthesized using the method reported in previous literature^[42]. 0.50 g of AgNO₃ and 0.36 g of Na₂HPO₄ are

added into two beakers, and 50 mL of water is appended separately to configure AgNO₃ aqueous solution (50 mL, 60 mM) and Na₂HPO₄ aqueous solution (50 mL, 20 mM). The aqueous solution of Na₂HPO₄ is gradually added drop by drop to the aqueous solution of AgNO₃ while stirring at room temperature for 3 h. The resulting golden precipitate is then obtained through repeated filtration and washing with distilled water. Lastly, the precipitate is dried overnight at 60°C to get Ag₃PO₄ powder, which is then stored at room temperature in the dark.

Results and discussion

Characterization of Ag₃PO₄ NPs

The morphology and particle size of Ag₃PO₄ NPs are observed by field emission scanning electron microscopy (FESEM). The morphology of Ag₃PO₄ NPs is close to spherical. The surface of Ag₃PO₄ NPs is not smooth and flat, made of a lot of tiny particles. This roughness can provide a larger surface area for interactions and catalytic reactions. As shown in Fig. 1c, the diameter of Ag₃PO₄ NPs particle size ranges from 300 to 900 nm. The average particle size of Ag₃PO₄ NPs is 500 nm. This uniform particle size distribution is beneficial for catalytic performance and reliable detection applications.

Laccase-mimicking activity of Ag₃PO₄ NPs

Laccase is a polyphenol oxidase that can catalyze many different phenolic compounds. Herein, different phenolic compounds such as 2,4-DP and phenol, are chosen as substrates to evaluate the laccase-mimicking activity of Ag₃PO₄ NPs (Fig. 2a). It is found that the Ag₃PO₄ NPs demonstrate remarkable activity in laccase-mimicking and possess the capability to catalyze the oxidation process of numerous phenolic compounds. Figure 2a indicates that the catalytical solution using 2,4-DP as substrate exhibits bright red (Sample 1), which has the highest characteristic absorption peak at 508 nm. Meanwhile, the solution adding phenol shows pink with a lower characteristic absorption peak at 508 nm (Sample 2). The solutions containing 3-aminophenol (Sample 3), 2-nitroresorcinol (Sample 4), and catechol (Sample 5) as substrates individually show pale yellow, brownish yellow, and light pink, which have relatively low characteristic absorption peaks at other wavelength positions. The results confirm that Ag₃PO₄ NPs possess good laccase-mimicking activity and can efficiently catalyze different phenolic substrates, in which 2,4-DP displayed the reddest color with the highest characteristic absorption peak. Therefore, 2,4-DP was used as the substrate to evaluate the laccase-mimicking of Ag₃PO₄ NPs in subsequent experiments.

Generally, oxygen is reduced to water during the catalytic reaction of laccase, serving as the electron acceptor in the oxidation process. To ascertain the significance of oxygen in the laccase-mimicking activity, the substrate 2,4-DP catalyzed by Ag₃PO₄ NPs under the conditions of air and nitrogen (N₂) is explored. Figure 2b shows that the color of the reaction solution under air conditions appears wine red and a distinct absorption peak is observable at 508 nm. On the contrary, the color of the solution under the N₂ condition shows lighter wine red and the absorption peak significantly decreases, which indicates that the laccase-mimicking catalytic reaction of Ag₃PO₄ NPs on phenolic compounds requires the participation of oxygen. Some studies have indicated that the reaction involving molecular oxygen can generate reactive oxygen species (ROS) with high oxidative capabilities, such as the superoxide anion radical (O₂⁻). Electron spin resonance (EPR) has been utilized to detect the production of O₂⁻ (Fig. 2c). The presence of six characteristic peaks corresponding to DMPO-O₂⁻ in a methanol dispersion of nanomaterials confirms the ability of Ag₃PO₄ NPs to produce O₂⁻.

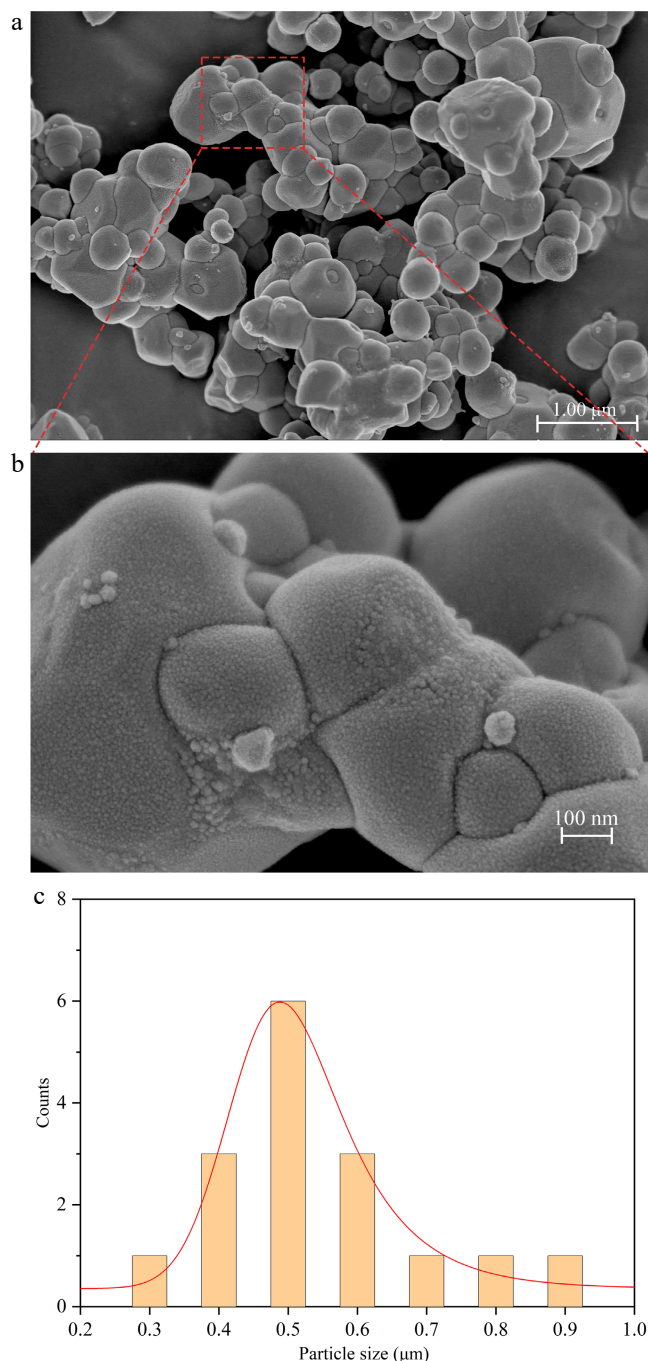


Fig. 1 (a), (b) Images of Ag_3PO_4 NPs captured by FE-SEM at various magnifications. (c) Particle size distribution of Ag_3PO_4 NPs.

The generated O_2^- can oxidize the phenol hydroxyl groups in phenolic compounds, leading to the formation of quinone radicals. These quinone radicals subsequently react with 4-AAP to generate red quinone imines.

Stability of Ag_3PO_4 NPs

The inactivation characteristics of natural enzymes at high temperatures or extreme pH levels limit their practical application. In contrast, Ag_3PO_4 NPs typically exhibit superior stability under these conditions. The effects of varying temperatures, ethanol concentrations, and salt concentrations on the enzymatic activity of Ag_3PO_4 NPs and natural laccase are explored.

As illustrated in Fig. 3a, Ag_3PO_4 NPs demonstrate high laccase-mimicking activity within the temperature range of 0–60 °C, indicat-

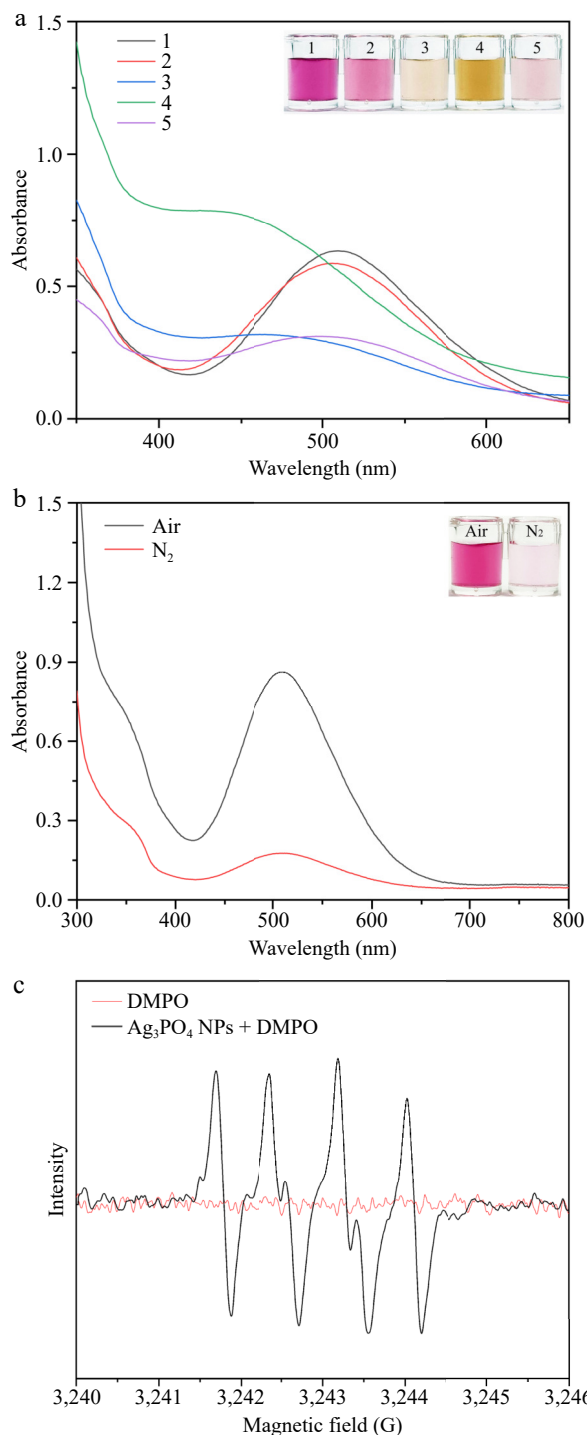


Fig. 2 (a) Visual images and the spectra of absorption for various reaction solutions. Sample 1: 2,4-DP; Sample 2: phenol; Sample 3: 3-aminophenol; Sample 4: 2-nitroresorcinol; Sample 5: catechol. (b) Color variation of the mixture containing 4-AAP, 2,4-DP, and Ag_3PO_4 NPs in Air- or N_2 -saturated buffers. (c) EPR spectra of O_2^- generated by Ag_3PO_4 NPs.

ing excellent thermal stability. When the temperature surpasses 40 °C, the catalytic activity of natural laccase diminishes, with relative activity decreasing significantly. At 80 °C, the relative activity of natural laccase is only 18.0%, substantially lower than that of Ag_3PO_4 NPs. Moreover, the influence of NaCl concentration on the catalytic performance of Ag_3PO_4 NPs and natural laccase is explored (Fig. 3b). Both Ag_3PO_4 NPs and natural laccase exhibit a rapid decline in

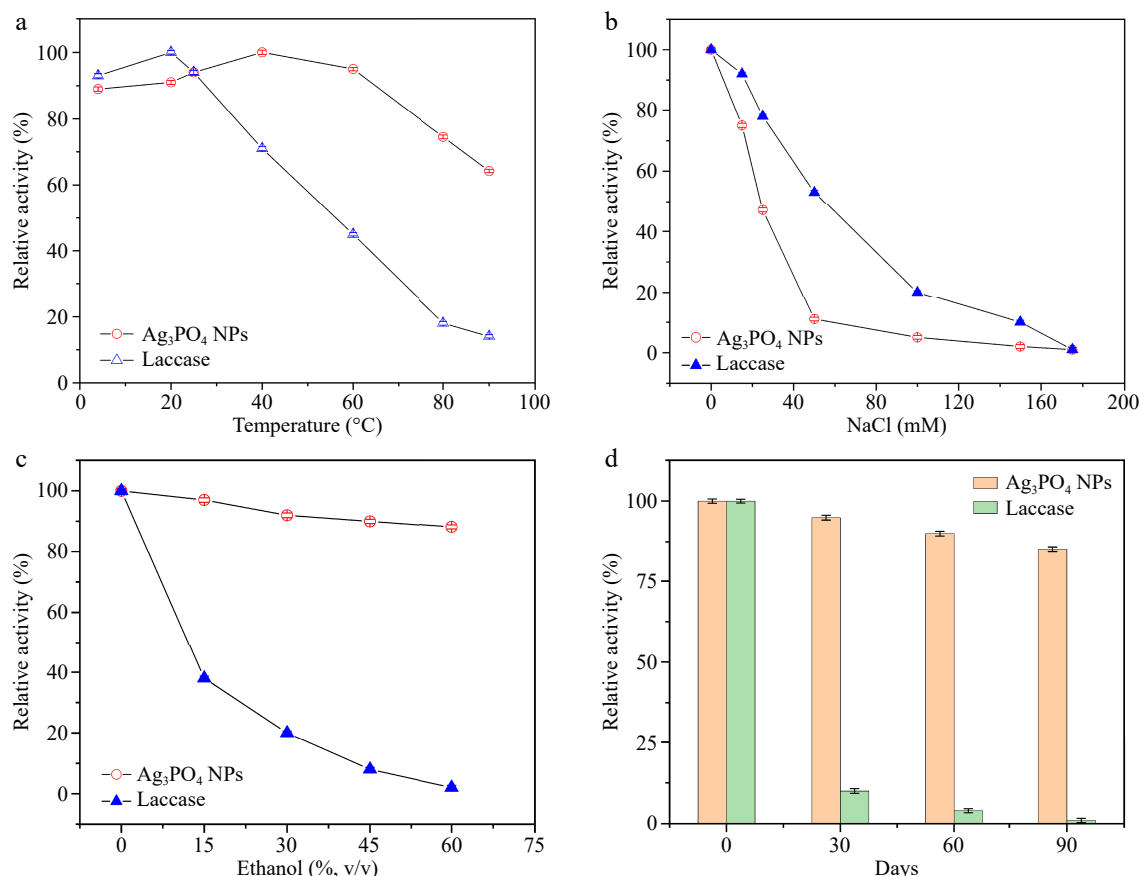


Fig. 3 (a) Impact of temperature on catalytic activity of Ag₃PO₄ NPs, and laccase. (b) Influence of NaCl concentration on laccase-mimicking catalytic activity of Ag₃PO₄ NPs. (c) Ethanol tolerance of Ag₃PO₄ NPs, and laccase. (d) Effect of long-term storage on catalytic activity of Ag₃PO₄ NPs and laccase.

catalytic activity as NaCl concentration increases. Notably, the relative activity of Ag₃PO₄ NPs decreases faster than that of natural laccase, suggesting that Ag₃PO₄ NPs have a lower tolerance to salt ions. Furthermore, the impact of different ethanol concentrations (0–60%) on the catalytic activity of Ag₃PO₄ NPs and natural laccase is proved. The data in Fig. 3c reveal that the catalytic activity of Ag₃PO₄ NPs remains relatively stable even as ethanol concentration increases, whereas the relative activity of natural laccase declines sharply and becomes almost entirely inactive at 60% ethanol concentration. These results confirm that Ag₃PO₄ NPs exhibit greater tolerance to organic solvents compared to natural laccase. Lastly, the storage stability of Ag₃PO₄ NPs is assessed in Fig. 3d. Ag₃PO₄ NPs maintain good stability over 90 d of storage, while the relative activity of laccase remains at 85.0%. As the storage duration increases, the relative activity of laccase decreases rapidly, dropping to 8.6% after 30 d and becoming almost completely deactivated after 90 d. These results indicate that Ag₃PO₄ NPs possess high stability and excellent storage stability across various conditions, along with enhanced tolerance to ethanol and salt ions. Compared to the costly and fragile natural laccase, the laccase-mimicking activity of silver phosphate nanoparticles is robust and stable, making it suitable for use in challenging environments.

Colorimetric detection of BPA

Principle of BPA detection

Ag₃PO₄ NPs possess excellent laccase-mimicking activity and can undoubtedly catalyze the oxidation of various phenolic substances like BPA. The principle of BPA detection is displayed in Fig. 4. Ag₃PO₄ NPs, exhibiting laccase-like activity, are capable of transferring electrons to dissolved oxygen in solution, resulting in the production of

O₂⁻ radicals. These radicals further oxidize BPA, leading to the formation of quinone radicals. Subsequently, the quinone radicals react with 4-AAP to generate red quinone imines, showing characteristic absorption peaks at 508 nm. The absorbance of the solution at 508 nm correlates directly with the concentration of BPA. Therefore, a new colorimetric strategy for BPA detection is successfully established based on the laccase-mimicking activity of Ag₃PO₄ NPs.

Feasibility of experiments

To ascertain the practicality of the developed colorimetric method for BPA detection, the spectral characteristics and corresponding hues of various solutions are reported. Figure 5a illustrates that Ag₃PO₄ NPs display robust laccase-mimicking activity, catalyzing the reaction between BPA and 4-AAP to produce the red product featuring a distinct absorption peak at 508 nm (Sample 1). As the BPA concentration decreases (Samples 2–4), the characteristic peak of the solution diminishes, accompanied by a shift in solution color from red to pale pink, ultimately approaching transparency. Notably, neither the individual substrates nor their pairwise combinations exhibit absorption at 508 nm (Fig. 5b). These findings suggest a direct correlation between the absorbance change (ΔA) at 508 nm of the solution and BPA concentration, enabling quantitative BPA detection.

Optimization of detection conditions

Effect of buffers pH

The pH of the system is important to maintain the activity and stability of Ag₃PO₄ NPs^[43]. Therefore, the effect of different HEPES buffer pH on BPA colorimetric detection is investigated. The results are displayed in Fig. 6a, which shows that the sensing signal gradually increases as pH rises. When pH is 7.5, the ΔA reaches the

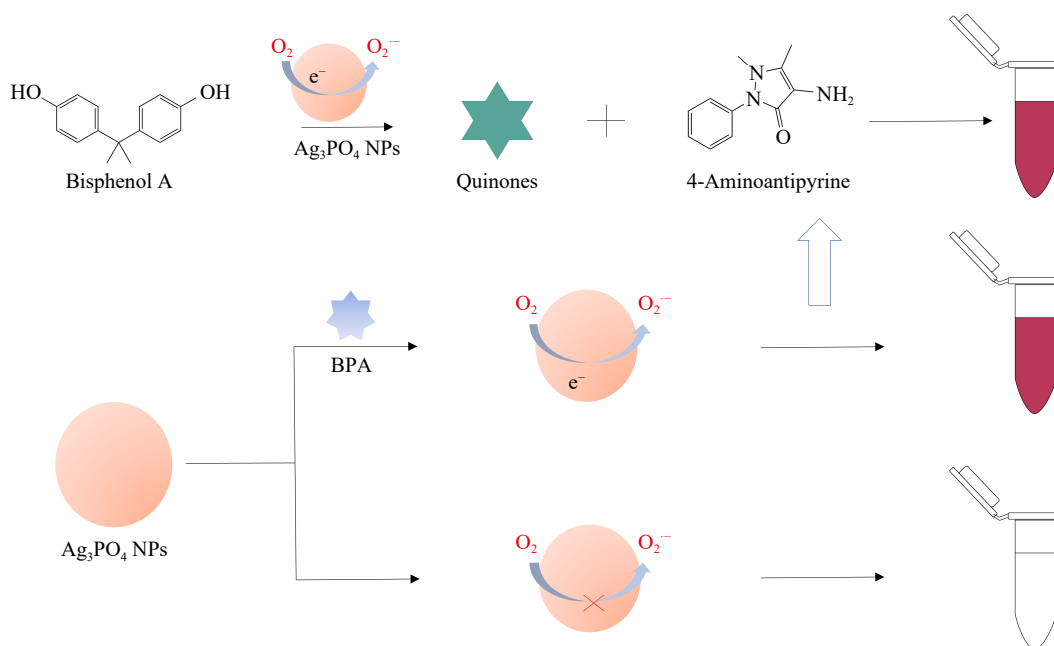


Fig. 4 Illustration of BPA detection using laccase-mimicking activity of Ag_3PO_4 NPs.

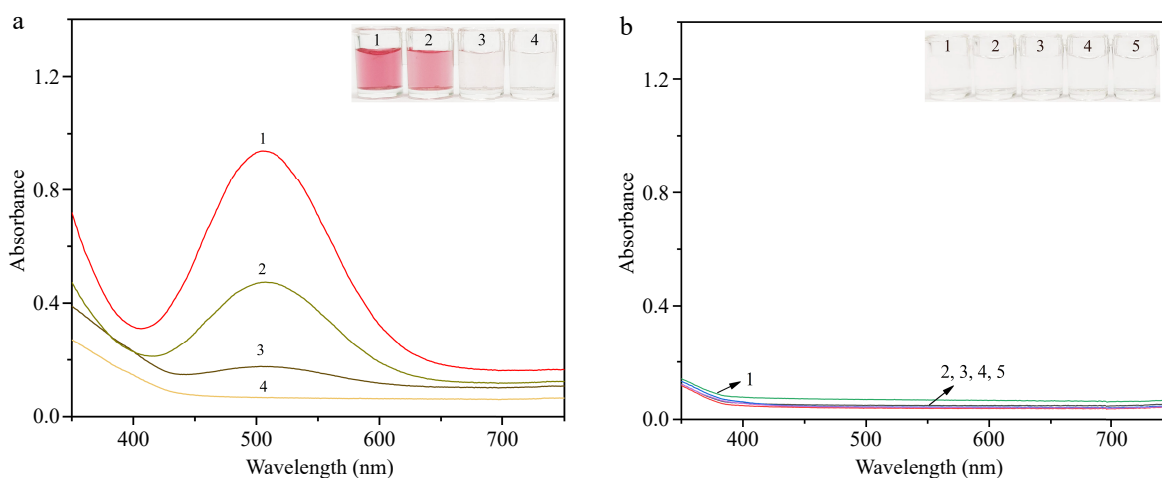


Fig. 5 (a) Visual representation and absorption spectrum profiles of solutions containing varied substances. Sample 1: Ag_3PO_4 NPs + $0.2 \text{ mg}\cdot\text{mL}^{-1}$ BPA + 4-AAP; Sample 2: Ag_3PO_4 NPs + $0.02 \text{ mg}\cdot\text{mL}^{-1}$ BPA + 4-AAP; Sample 3: Ag_3PO_4 NPs + $0.002 \text{ mg}\cdot\text{mL}^{-1}$ BPA + 4-AAP; Sample 4: Ag_3PO_4 NPs + 4-AAP. (b) Visual image and absorption spectra of the solution containing different substances. Sample 1: Ag_3PO_4 NPs; Sample 2: $0.2 \text{ mg}\cdot\text{mL}^{-1}$ BPA; Sample 3: 4-AAP; Sample 4: Ag_3PO_4 NPs + $0.2 \text{ mg}\cdot\text{mL}^{-1}$ BPA; Sample 5: $0.2 \text{ mg}\cdot\text{mL}^{-1}$ BPA + 4-AAP.

highest value. This is probably because pH 7.5 is more conducive to the binding of BPA to Ag_3PO_4 NPs. If the pH of the HEPES buffer continues to rise, the ΔA tends to decrease. Ag_3PO_4 NPs exhibit optimal stability within a specific pH range. Exceeding this range, the structural integrity of Ag_3PO_4 NPs can be destroyed or the surface charge state can be changed particularly at higher pH levels, leading to diminished catalytic activity and reducing binding efficiency of BPA to Ag_3PO_4 NPs. Meanwhile, the dissociation state of the phenolic compound is influenced by pH. Under alkaline conditions, BPA tends to dissociate more readily, which hinders its interaction with Ag_3PO_4 NPs. Furthermore, the excessive pH levels may increase the ionic strength of the solution, which also affects the electrostatic interactions and binding efficiency between Ag_3PO_4 NPs and BPA, consequently diminishing the signal strength.

Effect of buffer concentration

The effect of buffer concentration on BPA colorimetric detection is further investigated. The results are exhibited in Fig. 6b. When the

concentration of buffer solution is 20 mM, the ΔA at 508 nm reaches its maximum value. As the concentration of HEPES buffer solution increases, the ΔA shows a downward trend. The probable reason is that the higher concentration of buffer solution has a large number of ions, which will impede the transfer of electrons between Ag_3PO_4 NPs and dissolved oxygen.

Effect of 4-AAP concentration

The quinone generated by BPA under the catalysis of Ag_3PO_4 NPs will react with chromogenic agents like 4-AAP to produce red substances. Thus, 4-AAP has a great influence on the chromogenic reaction and color rendering effect. Herein, the effect of different 4-AAP quantities on BPA colorimetric detection is investigated (Fig. 6c). When the concentration of 4-AAP is 5 mM, the ΔA at 508 nm has a maximum value. Once the quantities of chromogenic agents surpass 5 mM, the absorbance tends to decrease, which is possibly due to background interference from high concentrations of 4-AAP.

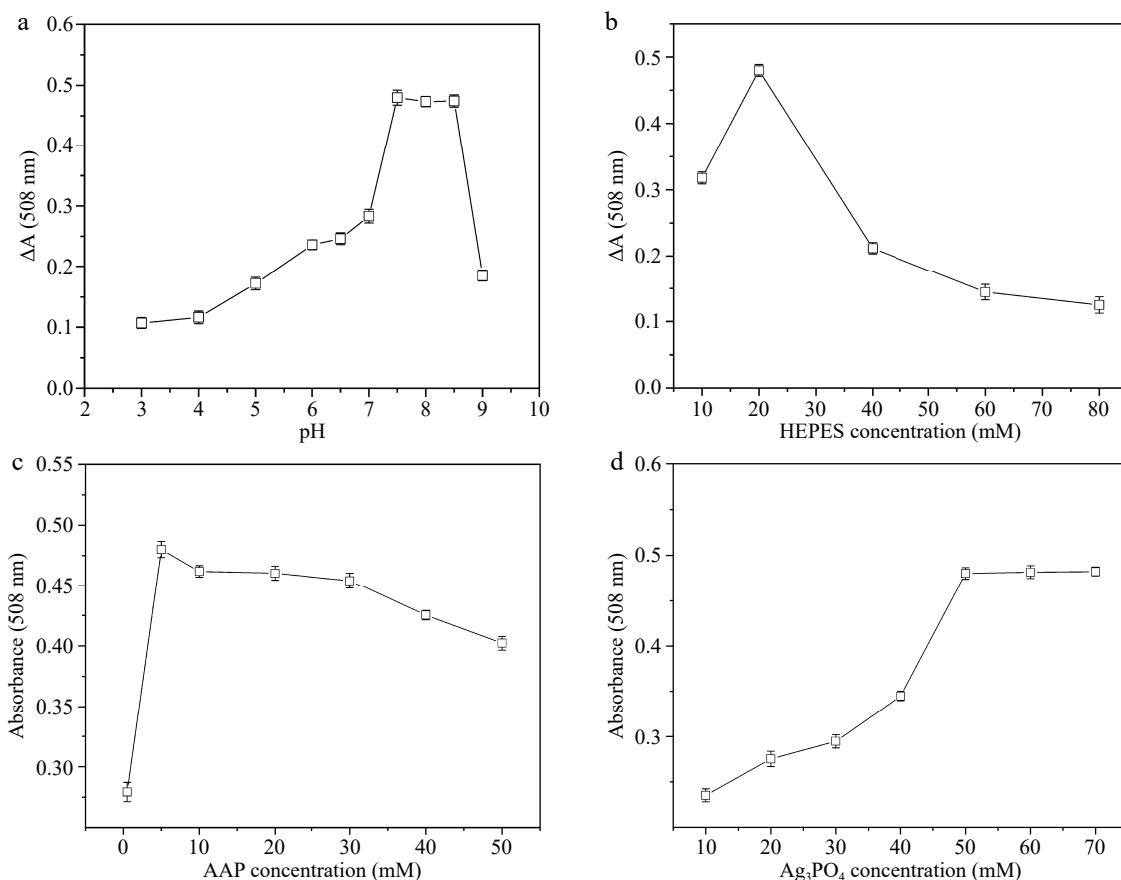


Fig. 6 Effect of (a) pH, (b) HEPES buffer concentration, (c) 4-AAP concentration, (d) Ag₃PO₄ NPs concentration on ΔA .

Effect of Ag₃PO₄ NPs concentration

The laccase-mimicking activity of Ag₃PO₄ NPs is the source of the sensing signal. The effects of different concentrations of Ag₃PO₄ NPs on BPA colorimetric detection are investigated. The results in Fig. 6d show that the ΔA of the sensing solution gradually increases with the increasing concentration of Ag₃PO₄ NPs from 10 to 50 $\mu\text{g}\cdot\text{mL}^{-1}$. The phenomenon may be that the binding of Ag₃PO₄ NPs to BPA has not yet reached saturation. When the content of Ag₃PO₄ NPs is 50 $\mu\text{g}\cdot\text{mL}^{-1}$, the ΔA reaches its maximum. Once the amount of Ag₃PO₄ NPs exceeds 50 $\mu\text{g}\cdot\text{mL}^{-1}$, the ΔA remains unchanged. This is probably because the binding of Ag₃PO₄ NPs and BPA has reached saturation.

Sensitivity

To evaluate the sensitivity of the colorimetric detection method, different quantities of BPA are added to the laccase-mimicking catalytic system of Ag₃PO₄ NPs solution under optimal conditions. As displayed in Fig. 7a, solutions with different quantities of BPA exhibit absorption peaks at 508 nm. The results indicate that ΔA at 508 nm of sensing solution decreases gradually with the decrease of BPA concentration. Therefore, the ΔA at 508 nm is measured and the limit of detection (LOD) is calculated. With the increase of BPA concentration, the color of the catalytic system gradually changes from colorless to dark red until the BPA quantity exceeds 200 $\text{mg}\cdot\text{L}^{-1}$ (Fig. 7b). If the concentration of BPA further increases, the ΔA remains unchanged. The linear range of the colorimetric sensing system is 0.6–40 $\text{mg}\cdot\text{L}^{-1}$, and the linear regression equation is $y = 0.020x + 0.009$ ($R^2 = 0.953$). The detection limit (LOD) of BPA is calculated as low as 0.222 $\text{mg}\cdot\text{L}^{-1}$, which is lower than the standards set by NHFPC (0.6 $\text{mg}\cdot\text{kg}^{-1}$) and FDA (1,000 $\text{mg}\cdot\text{kg}^{-1}$). The color of the solution turns red after 10 min, which can be used to determine the absorbance

value at 508 nm. In general, the colorimetric detection method for BPA utilizing the laccase-mimicking properties of Ag₃PO₄ NPs boasts fast analysis, ease of operation, and excellent stability, thereby fulfilling a wide range of practical application needs.

The performance of the developed colorimetric detection method is compared with that of previously established analytical methods (Table 1). The electrochemistry techniques exhibit superior performance in BPA detection, but they frequently necessitate intricate electrode manipulation and the use of sophisticated precision equipment. Although fluorescent sensors are highly sensitive, they often require complex material modifications. The aptamer-based sensing approaches demonstrate strong specificity. However, these techniques are costly and have difficulties in material recovery. In contrast, the colorimetric detection strategy based on Ag₃PO₄ NPs offers the benefits of simplicity, high sensitivity, cost-effectiveness, and environmental friendliness.

Selectivity

To assess the specificity of the colorimetric approach for detecting BPA, several phenolic compounds, glucose, heavy metal ions, metal ions, and amino acids are chosen as competitive targets. As shown in Fig. 8a, the solution containing BPA shows red, while the solution containing other competitive targets is colorless. The pure p-nitrophenol solution can not affect the result of BPA detection since its yellow-green color will become lighter after the laccase-mimicking catalytic reaction of Ag₃PO₄ NPs. Moreover, the ΔA at 508 nm of the solution added with BPA is significantly higher than those containing the same concentration of competitive targets. The results validate that the developed colorimetric system possesses outstanding selective recognition capabilities, which can be utilized for detecting BPA in actual samples.

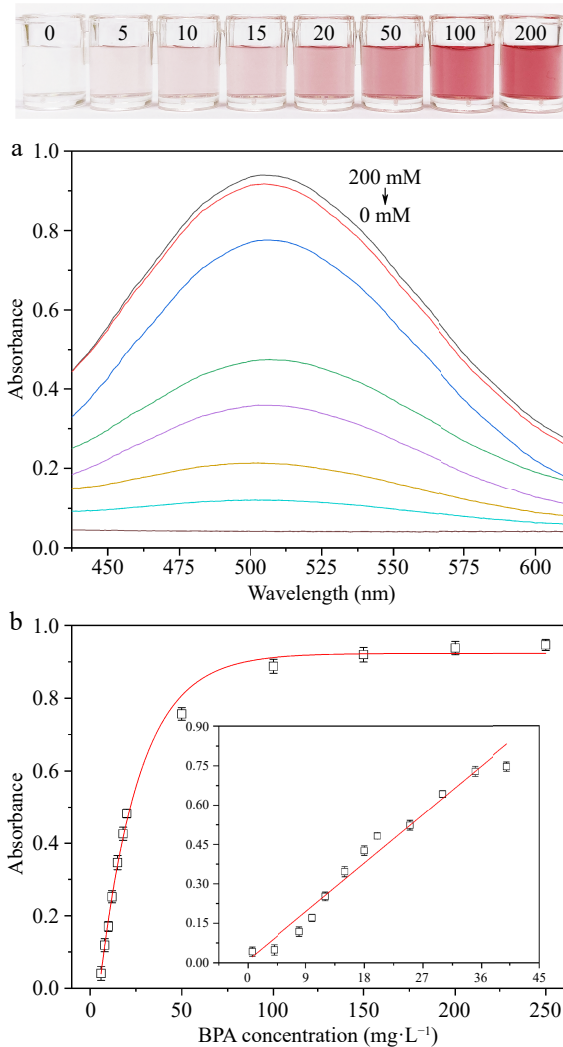


Fig. 7 (a) BPA sensitivity absorption spectrum. (b) Visual image and ΔA at 508 nm of the laccase-mimicking catalytic system added with different quantities of BPA.

As shown in Fig. 8b, phenolic compounds are organic compounds formed by direct connection of hydroxyl group (-OH) and aromatic nucleus (benzene ring or thick benzene ring). BPA consists of two benzene rings connected by a carbon-carbon bond in the middle, each of which has a hydroxyl group on the No. 4 carbon atom. This structure makes BPA have a certain reactivity. In the process of reaction with Ag_3PO_4 NPs, the hydroxyl group on carbon atom 4 of the benzene ring forms a relatively stable coordination bond with the metal Ag atom under the action of benzene ring conjugation and induction effect, which makes the binding with the catalytic active sites on the surface of Ag_3PO_4 NPs more firmly so that trigger the response. (Fig. 8c) Therefore, we hypothesize that BPA has this special structure and can be used as a target for specific reactions with Ag_3PO_4 NPs. However, most of the targets (such as metal ions, amino acids, etc.) are not phenolic compounds so they do not have the phenol hydroxyl group catalyzed by Ag_3PO_4 NPs and do not participate in the response.

p-nitrophenol has only one benzene ring, and the substituted group on the benzene ring is the nitro (-NO₂), not the hydroxyl group. In terms of reactivity, the nitro-substituted group of p-nitrophenol may reduce the reactivity of the phenol hydroxyl group, making it less efficient to react with silver phosphate. In terms of electron transfer, nitro is a strong electron-absorbing group, which

Table 1. Comparison of similar methods for BPA detection.

Methods	Linear range ($\mu\text{mol} \cdot \text{L}^{-1}$)	LOD ($\mu\text{mol} \cdot \text{L}^{-1}$)	Ref.
Electrochemistry	0.05–5; 5–30	0.006	[44]
Fluorogenic sensing	0.001–1; 5–100	3.5	[45]
Aptamer sensor	0.02–5	0.008	[46]
Colorimetry (this work)	26.3–88.1	2.4	

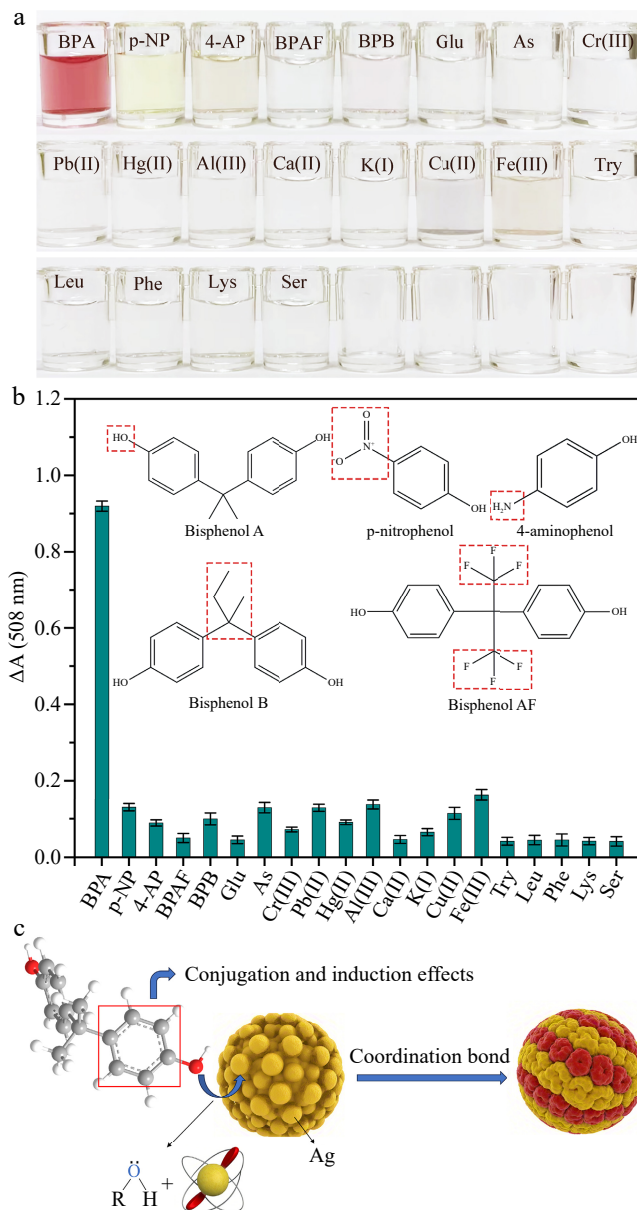


Fig. 8 (a), (b) Visual image and ΔA at 508 nm of the laccase-mimicking catalytic system added with 0.2 $\text{mg} \cdot \text{mL}^{-1}$ of BPA and different competitive substances. (c) Schematic illustration of the coordination between BPA and Ag_3PO_4 NPs.

can affect the electron distribution on the benzene ring. Hydroxyl groups in BPA may be more likely to transfer electrons to silver phosphate, triggering a subsequent chain of oxidation reactions. However, the nitro-substituents of p-nitrophenol may hinder the effective transfer of electrons, resulting in the reaction of p-nitrophenol with Ag_3PO_4 NPs. As for steric hindrance, the catalytic active sites of Ag_3PO_4 NPs may have a certain spatial configuration, which makes it easier for some compounds to bind to them. The benzene

rings and hydroxyl groups in BPA may just meet the spatial requirements of the active sites of silver phosphate catalysis, which makes it easier to react. However, the nitro-substituents of p-nitrophenol increase its steric hindrance, which makes it difficult to effectively bind to the catalytic active sites of Ag_3PO_4 NPs.

Although the structure of 4-aminophenol also contains a benzene ring and a hydroxyl functional group, the hydroxyl group is connected to an amino ($-\text{NH}_2$) functional group at the parapet (position 4) of the benzene ring, rather than another benzene ring-like BPA. Bisphenol AF, a fluorinated derivative of BPA, has hydrogen atoms in one or more benzene rings of bisphenol AF (usually at the benzene ring position opposite the hydroxyl group) replaced by fluorine atoms, which are also a strong electron-withdrawing group, possibly. Bisphenol B consists of two benzene rings connected by a carbon chain of three carbon atoms (usually an isopropyl group), but they are connected in different ways and locations. The structural differences of these three phenolic compounds will also affect the effective binding to the silver phosphate catalytic active sites in terms of reactivity, electron transport, and steric hindrance.

Recyclability of Ag_3PO_4 NPs

The recyclability of the laccase-mimicking activity of Ag_3PO_4 NPs has been extensively investigated. It has been observed that the Ag_3PO_4 NPs retain functionality after multiple cycles, maintaining approximately 85% of laccase-mimicking catalytic activity even after seven cycles (Fig. 9). The remarkable recyclability enhances the applicability of colorimetric sensing systems in diverse practical settings.

Analysis of BPA residues in actual samples

Because BPA is often present in food contact materials, some food water samples like tap water and bottled water are selected as actual samples to verify the practical application of colorimetric detection for BPA. However, it is difficult to obtain actual samples containing BPA in daily life, because BPA usually migrates from plastic products to food raw materials under high temperature and pressure^[47]. Therefore, we have supplemented bottled honey treated with high temperatures. Additionally, the solutions of bottled honey are subsequently diluted tenfold with ultra-pure water for analysis of the actual samples. Table 2 shows that the calculated average recovery of BPA ranges from 91.0%–101.0% with a relative standard deviation (RSD) of 3.5%–6.2%. In comparison to standard techniques such as LC-MS/MS, the results show that the established colorimetric strategy has excellent practicability, and can be applied as an alternative strategy for BPA detection in actual samples.

Conclusions

In summary, Ag_3PO_4 NPs with excellent laccase-mimicking activity are successfully synthesized by a facile coprecipitation method, which is first employed to establish a colorimetric method for BPA detection. With the aid of the 4-AAP, Ag_3PO_4 NPs are capable of oxidizing BPA to produce wine-red quinone imines, which display a distinct absorption peak at 508 nm. Ag_3PO_4 NPs can transfer electrons to dissolved oxygen and produce $\text{O}_2^{\cdot-}$ in solution, which further oxidizes BPA to generate quinone radicals. The absorbance at 508 nm of the solution varies directly with the BPA concentration. Overall, the proposed method boasts several notable innovations and advantages. Firstly, Ag_3PO_4 NPs have the advantages of strong stability, mass production, and low cost. Secondly, the colorimetric method has the advantages of high selectivity, fast, real-time, and efficient detection results, and can be distinguished by visual senses alone. Finally, the colorimetric method can also be applied to the

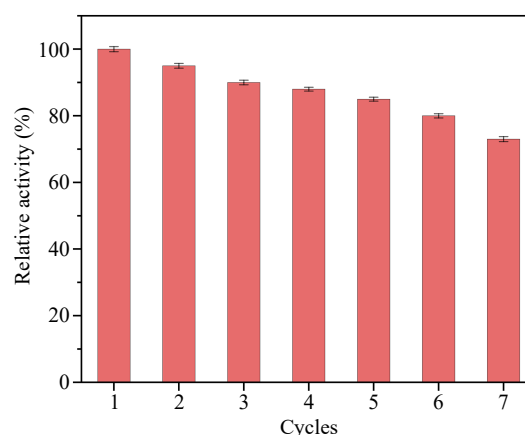


Fig. 9 The recyclability of Ag_3PO_4 NPs. The activity of 100% is set where absorbance is highest and the relative activities of other samples are calculated based on this standard. The Ag_3PO_4 NPs are recovered through centrifugation at 10,000 rpm for 10 min, washed with double-distilled water, and then re-disperse.

Table 2. Determination of BPA in actual samples.

Sample	Spiked ($\text{mg}\cdot\text{L}^{-1}$)	This method			LC-MS/MS		
		Found ($\text{mg}\cdot\text{L}^{-1}$)	Recovery (%)	RSD (%)	Found ($\text{mg}\cdot\text{L}^{-1}$)	Recovery (%)	RSD (%)
Tap water	10.0	9.1	91.0	3.5	8.3	83.0	3.7
	20.0	19.5	97.5	4.7	18.7	93.5	3.2
	30.0	29.3	97.7	6.2	29.6	98.7	4.5
Bottled water	10.0	9.4	94.0	4.9	8.7	87.0	2.7
	20.0	19.0	95.0	3.8	18.5	92.5	3.3
	30.0	28.4	94.7	5.1	29.3	97.7	5.0
Bottled honey	10.0	9.7	97.0	5.8	9.2	92.0	2.9
	20.0	20.2	101.0	4.9	18.9	94.5	3.6
	30.0	28.9	96.3	6.0	29.2	97.3	5.5

quantitative detection of BPA. These characteristics render colorimetric sensors highly suitable for real-time monitoring and rapid analysis. Owing to strong stability, ease of mass production, low cost, and excellent recyclability, Ag_3PO_4 NPs hold significant potential for widespread application in the food detection of BPA, which offers a new approach to detecting phenolic contaminants.

Author contributions

The authors confirm contribution to the paper as follows: investigation: Wu S, Chen J; validation: Wu S, Tang Y; methodology, data curation, writing - original draft: Wu S; formal analysis: Chen J, Yang Y; supervision: Chen J, Tang Y, Wu Y; funding acquisition, project administration, writing - review & editing: Wu Y. All authors reviewed the results and approved the final version of the manuscript.

Data availability

The data supporting the findings of this study are available upon reasonable request from the corresponding author. All relevant data generated or analyzed during this study have been included in this published article.

Acknowledgments

This work was financially supported by the National Natural Science Foundation of China (32360621, 32160603, 31760486), the

Guizhou Provincial Basic Research Program (ZK[2021]Key Project 037), the Guizhou Provincial Key Technology R&D Program (QKHZC[2023]123).

Conflict of interest

The authors declare that they have no known competing financial interests or personal relationships that could have appeared to influence the work reported in this paper.

Dates

Received 17 October 2024; Revised 21 December 2024; Accepted 17 January 2025; Published online 20 February 2025

References

- Im J, Löffler FE. 2016. Fate of bisphenol A in terrestrial and aquatic environments. *Environmental Science & Technology* 50:8403–16
- Michałowicz J. 2014. Bisphenol A – sources, toxicity and biotransformation. *Environmental Toxicology and Pharmacology* 37:738–58
- Bhatnagar A, Anastopoulos I. 2017. Adsorptive removal of bisphenol A (BPA) from aqueous solution: a review. *Chemosphere* 168:885–902
- Xiao Z, Wang R, Suo D, Li T, Su X. 2020. Trace analysis of bisphenol A and its analogues in eggs by ultra-performance liquid chromatography-tandem mass spectrometry. *Food Chemistry* 327:12688
- Zeng N, Wang X, Dong Y, Yang Y, Yin Y, et al. 2023. Aptasensor based on screen-printed carbon electrodes modified with CS/AuNPs for sensitive detection of okadaic acid in shellfish. *Journal of Analysis and Testing* 7:128–35
- Yang Y, Zhang X, Wang X, Jing X, Yu L, et al. 2024. Self-powered molecularly imprinted photoelectrochemical sensor based on Ppy/QD/HOF heterojunction for the detection of bisphenol A. *Food Chemistry* 443:138499
- Lim HJ, Lee EH, Lee SD, Yoon Y, Son A. 2018. Quantitative screening for endocrine-disrupting bisphenol A in consumer and household products using NanoAptamer assay. *Chemosphere* 211:72–80
- Hwang E, Lee B. 2022. Synthesis of a fluorescence sensor based on carbon quantum dots for detection of bisphenol A in aqueous solution. *Korean Journal of Chemical Engineering* 39:1324–32
- Kadam VV, Balakrishnan RM, Ettiyappan JP. 2021. Fluorometric detection of bisphenol A using β -cyclodextrin-functionalized ZnO QDs. *Environmental Science and Pollution Research* 28:11882–92
- Wang YQ, Chen TT, Zhang HM. 2010. Investigation of the interactions of lysozyme and trypsin with bisphenol A using spectroscopic methods. *Spectrochimica Acta Part A: Molecular and Biomolecular Spectroscopy* 75:1130–37
- Liu SG, Wu T, Liang Z, Zhao Q, Gao W, et al. 2023. A fluorescent method for bisphenol A detection based on enzymatic oxidation-mediated emission quenching of silicon nanoparticles. *Spectrochimica Acta Part A: Molecular and Biomolecular Spectroscopy* 302:123123
- Pan Y, Wu M, Shi M, Shi P, Zhao N, et al. 2023. An Overview to Molecularly Imprinted Electrochemical Sensors for the Detection of Bisphenol A. *Sensors* 23:8656
- Tan F, Cong L, Li X, Zhao Q, Zhao H, et al. 2016. An electrochemical sensor based on molecularly imprinted polypyrrole/graphene quantum dots composite for detection of bisphenol A in water samples. *Sensors and Actuators B: Chemical* 233:599–606
- Piao MH, Noh HB, Rahman MA, Won MS, Shim YB. 2008. Label-free detection of bisphenol A using a potentiometric immunosensor. *Electroanalysis* 20:30–37
- Palchetti I, Mascini M. 2012. Electrochemical nanomaterial-based nucleic acid aptasensors. *Analytical And Bioanalytical Chemistry* 402:3103–14
- Liu W, Li M, Zhang P, Jiang H, Liu W, et al. 2024. One-step growth of Cu-doped carbon dots in amino-modified carbon nanotube-modified electrodes for sensitive electrochemical detection of BPA. *Microchimica Acta* 191:309
- Hui Y, Webster RD. 2011. Absorption of water into organic solvents used for electrochemistry under conventional operating conditions. *Analytical Chemistry* 83:976–81
- Jesuraj R, Amalraj A, Vaidyanathan VK, Perumal P. 2023. Exceptional peroxidase-like activity of an iron and copper based organic framework nanosheet for consecutive colorimetric biosensing of glucose and kanamycin in real food samples. *Analyst* 148:5157–71
- Rao H, Xue X, Luo M, Liu H, Xue Z. 2021. Recent advances in the development of colorimetric analysis and testing based on aggregation-induced nanozymes. *Chinese Chemical Letters* 32:25–32
- Tang D, Shi J, Wu Y, Luo H, Yan J, et al. 2023. Flexible self-powered sensing system based on novel DNA circuit strategy and graphdiyne for thalassemia gene by rapid naked-eye tracking and open-circuit voltage. *Analytical Chemistry* 95:16374–82
- Song Y, Wang Z, Wu Q, Su J, Liao J, et al. 2025. A dual-mode strategy for early detection of sugarcane pokkah boeng disease pathogen: a portable sensing device based on Cross-N DNA framework and MoS₂@GDY. *Biosensors & Bioelectronics* 267:116874
- Shi J, Li P, Huang Y, Wu Y, Wu J, et al. 2024. Smartphone-assisted self-powered dual-mode biosensor designed on binary 3D DNA Walkers mediated CRISPR/Cas12a system. *Chemical Engineering Journal* 483:149231
- Bayram A, Horzum N, Metin AU, Kılıç V, Solmaz ME. 2018. Colorimetric bisphenol-A detection with a portable smartphone-based spectrometer. *IEEE Sensors Journal* 18:5948–55
- Ren S, Cho S, Lin RX, Gedi V, Park S, et al. 2022. Nonbiodegradable spiegelmer-driven colorimetric biosensor for bisphenol A detection. *Biosensors* 12:864
- Xu J, Li Y, Bie J, Jiang W, Guo J, et al. 2015. Colorimetric method for determination of bisphenol A based on aptamer-mediated aggregation of positively charged gold nanoparticles. *Microchimica Acta* 182:2131–38
- Lee EH, Lee SK, Kim MJ, Lee SW. 2019. Simple and rapid detection of bisphenol A using a gold nanoparticle-based colorimetric aptasensor. *Food Chemistry* 287:205–13
- Huang A, Xia L, Chen J, Wu S, Tang Y, et al. 2024. A dual-mode colorimetric and fluorometric sensor for the detection of spermine and spermidine in food based on N-doped carbon dots and peroxidase-like activity of V₆O₁₃ nanobelts. *Sensors and Actuators B: Chemical* 409:135596
- Giardina P, Faraco V, Pezzella C, Piscitelli A, Vanhulle S, et al. 2010. Laccase: a never-ending story. *Cellular and Molecular Life Sciences* 67:369–85
- Zhu Y, Zhou Z. 2021. The genotype-specific laccase gene expression and lignin deposition patterns in apple root during Pythium ultimum infection. *Fruit Research* 1:12
- Antošová Z, Sychrová H. 2016. Yeast hosts for the production of recombinant laccases: a review. *Molecular Biotechnology* 58:93–116
- Ning N, Tan H, Sun X, Ni J. 2017. Advance of heterologous expression study of eukaryote-origin laccases. *Chinese Journal of Biotechnology* 33:565–77
- Ma H, Zheng N, Chen Y, Jiang L. 2021. Laccase-like catalytic activity of Cu-tannic acid nanohybrids and their application for epinephrine detection. *Colloids and Surfaces A: Physicochemical and Engineering Aspects* 613:126105
- Jiao J, Yang X, Jin LN, Gao J, Zhou Y, et al. 2016. Conservative and variability of the important functional sites in a laccase from *Bacillus subtilis*. *Chemical Journal of Chinese Universities* 37(7):1320–27
- Gao LZ, Yan XY. 2013. Discovery and current application of nanozyme. *Progress In Biochemistry And Biophysics* 40:892–902
- Niu J, Sun S, Liu P, Zhang X, Mu X. 2023. Copper-based nanozymes: properties and applications in biomedicine. *Journal of Inorganic Materials* 38(5):489–502
- Amalraj A, Narayanan M, Perumal P. 2022. Highly efficient peroxidase-like activity of a metal-oxide-incorporated CeO₂-MIL(Fe) metal-organic framework and its application in the colorimetric detection of melamine and mercury ions via induced hydrogen and covalent bonds. *Analyst* 147:3234–47

37. Yang L, Guo XY, Zheng QH, Zhang Y, Yao L, et al. 2023. Construction of platinum nanozyme by using carboxymethylcellulose with improved laccase-like activity for phenolic compounds detection. *Sensors and Actuators B: Chemical* 393:134165
38. Chen Z, Li S, Yang F, Yue W. 2024. Construction of a colorimetric sensor array for the identification of phenolic compounds by the laccase-like activity of N-doped manganese oxide. *Talanta* 268:125324
39. Yin Q, Wang Y, Yang D, Yang Y, Zhu Y. 2024. A colorimetric detection of dopamine in urine and serum based on the CeO₂@ZIF-8/Cu-CDs laccase-like nanozyme activity. *Luminescence* 39:e4684
40. Wang P, Chen R, Jia Y, Xu Y, Bai S, et al. 2024. Cu-chelated polydopamine nanozymes with laccase-like activity for photothermal catalytic degradation of dyes. *Journal of Colloid and Interface Science* 669:712–22
41. Wang J, Huang R, Qi W, Su R, He Z. 2022. Preparation of amorphous MOF based biomimetic nanozyme with high laccase- and catecholase-like activity for the degradation and detection of phenolic compounds. *Chemical Engineering Journal* 434:134677
42. Niu X, He H, Ran H, Wu Z, Tang Y, et al. 2023. Rapid colorimetric sensor for ultrasensitive and highly selective detection of Fumonisin B₁ in cereal based on laccase-mimicking activity of silver phosphate nanoparticles. *Food Chemistry* 429:136903
43. Jadhav SB, Singhal RS. 2014. Laccase-gum Arabic conjugate for preparation of water-soluble oligomer of catechin with enhanced antioxidant activity. *Food Chemistry* 150:9–16
44. Alam AU, Deen MJ. 2020. Bisphenol A Electrochemical Sensor Using Graphene Oxide and β -Cyclodextrin-Functionalized Multi-Walled Carbon Nanotubes. *Analytical Chemistry* 92:5532–39
45. Ribes A, Aznar E, Bernardos A, Marcos MD, Amorós P, et al. 2017. Fluorogenic sensing of carcinogenic bisphenol A using aptamer-capped mesoporous silica nanoparticles. *Chemistry-a European Journal* 23:8581–84
46. Kuang H, Yin H, Liu L, Xu L, Ma W, et al. 2014. Asymmetric plasmonic aptasensor for sensitive detection of bisphenol A. *ACS Applied Materials & Interfaces* 6:364–69
47. Abraham A, Chakraborty P. 2020. A review on sources and health impacts of bisphenol A. *Reviews on Environmental Health* 35:201–10



Copyright: © 2025 by the author(s). Published by Maximum Academic Press on behalf of China Agricultural University, Zhejiang University and Shenyang Agricultural University. This article is an open access article distributed under Creative Commons Attribution License (CC BY 4.0), visit <https://creativecommons.org/licenses/by/4.0/>.